Novel ultrahard sp2/sp3 hybrid carbon allotrope from crystal chemistry and first principles: Body-centered tetragonal C6 ('neoglitter')

Samir Matar, Vladimir Solozhenko

Novel ultrahard sp^2/sp^3 hybrid carbon allotrope from crystal chemistry and first principles: body-centered tetragonal C_6 ('neoglitter')

Samir F. Matar[1] and Vladimir L. Solozhenko[2,*]

[1] Lebanese German University (LGU), Sahel Alma, Jounieh, Lebanon

https://orcid.org/0000-0001-5419-358X

[2] LSPM–CNRS, Université Sorbonne Paris Nord, 93430 Villetaneuse, France

https://orcid.org/0000-0002-0881-9761

Abstract:

A novel ultrahard carbon allotrope, body-centered tetragonal C_6 (space group *I*-4*m*2) presenting mixed sp^2/sp^3 carbon hybridizations is proposed by crystal chemistry approach and studied for the ground state structure and stability (both dynamic and mechanical) within density functional theory (DFT). The structure characterized by *C4* tetrahedra connected with C–C trigonal carbons shows close relationship with C_6 'glitter' devised about 30 years ago. While 'glitter' has underlying net labeled '**tfi**' according to RCSR nomenclature, novel C_6 called 'neoglitter' is identified as '**tfa**' underlying net. 'Neoglitter' is characterized by large bulk and shear moduli approaching those of diamond, and very high Vickers hardness (H_V = 85 GPa). High phonons frequencies ω ~ 40 THz, close to diamond, are observed and attributed to trigonal C-C pairs stretching. The electronic band structure points to metallic-like behavior assigned mainly to the itinerant role of trigonal carbon π-electrons. The presence of both trigonal (sp^2) and tetrahedral (sp^3) carbon in 'neoglitter' is relevant to an extensive research domain involving nanodiamonds and various electronic applications.

* Corresponding author (vladimir.solozhenko@univ-paris13.fr)

1. Introduction

Diamond, as natural gem and man-made for applications [1] is recognized as the hardest material. The basic reason for extreme hardness is the three-dimensional arrangement of carbon in corner sharing *C4* tetrahedra with d(C–C) = 1.55 Å, i.e., the sum of two *r*(C) = 0.77 Å atomic radii, making a perfectly covalent network. In recent decades many research efforts were focused on the identification of new ultrahard carbon allotropes mimicking structure through predicting software such as CALYPSO [2] and USPEX [3] complementarily with first principles calculations carried out mainly within the well-established quantum mechanics framework of the density functional theory (DFT) [4,5]. In this context the SACADA database (SACADA 3D) [6] regroups all known carbon allotropes thus helping researchers in their endeavor. Recently we reported body-centered tetragonal C_4 (Fig. 1a) proposed in space group *I*-4*m*2 as seed to build larger carbon networks and to serve as a template for other original chemical compounds [7]. C_4 was then identified with '**dia**' (diamond) topology by *TopCryst* software [8]. Crystal chemistry modification of central carbon coordinates led to tetragonal C_6 characterized by mixed $C(sp^2)/C(sp^3)$ hybridizations (Fig. 1b). The transformation from C_4 to C_6 is sketched in Fig. 1c.

The same C_6 stoichiometry identifies 'glitter', carbon allotrope proposed earlier as a dense tetragonal hexacarbon starting *ad hoc* from 1,4-cyclohexadienoid units [9]. The corresponding structure shown in Fig. 1d consists of four trigonal carbons: $C(sp^2)$ and two tetrahedral carbons: $C(sp^3)$. This structure characterized as '**tfi**' (SACADA #95) [6] was called 'glitter', i.e., *shining*, due to the electronic conductivity. First principles investigations and full characterization of 'glitter' C_6 was recently undertaken, and the structure was used as a template to propose novel equiatomic SiCN [10] and BCN [11]. The established relationship between 'glitter' C_6 and the proposed tetragonal C_6 allowed us to call the latter a 'neoglitter'.

2. Computational framework

The search for the ground state energies, ground state structures and related mechanical and dynamic properties was carried out within DFT with Vienna Ab initio Simulation Package (VASP) code [12,13] using the projector augmented wave (PAW) method [13,14] for the atomic potentials with all valence states (especially in regard of such light element as carbon). The exchange-correlation effects inherent to DFT were considered with the generalized gradient approximation (GGA) following Perdew, Burke, and Ernzerhof [15]. We note here that the PBE functional underestimates band gap values due to the common self-interaction error in electronic properties, and hybrid functionals such as the HSE06 (Heyd, Scuseria, and Ernzerhof) one [16] are used to overcome these limitations. However, for the present carbon allotrope, which was found to be a conductor similar to the previously studied 'glitter', further calculations using the HSE06 hybrid functional did not lead to significant changes in the GGA results. Other calculations using the

hybrid HSE06 functional [16] did not result in significant changes of the GGA results. Relaxing the atoms onto the ground state structures was carried out with the conjugate-gradient algorithm [17]. The tetrahedron method was applied for both geometry relaxation and total energy calculations using Blöchl *et al*. corrections [18] and Methfessel-Paxton scheme [19]. Brillouin-zone integrals were approximated using a special k-point sampling of Monkhorst and Pack [20]. The optimization of the structural parameters was performed until the forces on the atoms were less than 0.02 eV/Å and all stress components below 0.003 eV/Å^3. The calculations were converged at an energy cut-off of 400 eV for the plane-wave basis set regarding the k-point integration in the reciprocal space up to 12×12×12 k_x,k_y,k_z for the final convergence and relaxation to zero strains. In the post-treatment process of the ground state electronic structures, the charge density projections were operated onto the carbon atomic sites. The elastic constants C_{ij} and the phonon band structures were calculated to assess the mechanical and dynamic stabilities. Calculations of phonon dispersion curves were also carried out to verify the dynamic stability of the novel carbon allotrope. The phonon modes were computed via finite displacements of the atoms off their equilibrium positions to obtain the forces from the summation over the different configurations. The phonon bands along the direction of the Brillouin zone were subsequently obtained using "*phonopy*" code based on Python language [21]. The electronic band structure and the site projected density of states (DOS) of C_6 were obtained using the all-electrons DFT-based augmented spherical method (ASW) [22].

3. Results and Discussion

Table 1 shows the crystal structure parameters of '**dia**' C_4 [7]. The atomic coordinates are all general positions and related to diamond. The change to C_6 is operated at the two-fold (2*d*) ½, 0, ¼ transforming to four-fold (4f) 0, ½, z. Full geometry relaxation onto ground state structure leads to C_6 (Fig. 1b) inscribed in the same body-centered tetragonal space group *I*-4*m*2. Table 1 shows the crystal parameters of C_6 characterized with a larger volume expected from the spacing between *C4* tetrahedra as schematized in Fig. 1c. Common C1 positioned at corners and body center features both carbon structures but the introduction of C2-C2 pairs is represented by the change from two-fold (2d) in tet-C_4 to four-fold (4f) in tet-C_6. The interatomic distances are very close in both structures. The trend of cohesive energy per atom obtained after full geometry relaxation onto ground state is a decrease from $E_{total/atom}$ (C_4) = -2.4 eV to $E_{total/atom}$ (C_6) = -1.7 eV. Such trend is explained by the loss of the homogeneous 3D corner sharing *C4* tetrahedra observed in diamond-like C_4 in contrast to C_6. Nevertheless, 'neoglitter' remains cohesive, and as shown below, it is stable both mechanically (elastic properties) and dynamically (phonons).

Comparing the two tetragonal C_6 allotropes, we should say that whereas 'glitter' was devised from modeling an organic molecule inscribed in a tetragonal cage (*ad hoc*), presently proposed 'neoglitter' C_6 is structurally derived from diamond expressed as C_4. Simulated X-ray diffraction patterns of three carbon allotropes ('glitter', 'neoglitter' and diamond) are shown in Fig. 2. The

observed differences of diffraction lines intensities of 'glitter' and 'neoglitter' are likely related to the different topologies of these two structures identified by *TopCryst* analysis program [8] as '**tfi**' and '**tfa**' i.e., **dia-**derived in RCSR (Reticular Chemistry Structure Resource) nomenclature.

Charge density analyses.

As further illustration of the above-mentioned energy trends, we analyzed difference between C_4 and 'neoglitter' C_6 considering the charge density resulting from the calculations.

The corresponding projections of the charge density onto the atoms and bonds are shown in Fig. 3 with yellow volumes using multicell for the sake of extended views with the structure sketches and with a polyhedral view in left-hand-side and right-hand side representations, respectively. The trigonal character of C2-C2 pairs is also shown with a substantial charge density. But the most representative of the charge density difference between the two structures is observed in the change from a purely covalent system in tet-C_4 where the charge density is localized on each C atom with tetrahedra shape, to tet-C_6 where there is a continuous density charge from C1 (tetrahedral) to C2 (trigonal) allowing us to suggest a transition from the insulator (diamond) to a conductor. Indeed, the analysis of the electronic band structure in the subsection below will show such a result.

Mechanical properties

(i) *Elastic constants*

The investigation of mechanical characteristics was based on the calculations of elastic properties determined by performing finite distortions of the lattice and deriving the elastic constants (C_{ij}) from the strain–stress relationship. It is well-known that most of solids are polycrystalline and can be considered to a large extent as randomly oriented single-crystalline grains. Therefore, they may be described by bulk (B) and shear (G) moduli obtained by averaging the single-crystal elastic constants. The method used here is Voigt's [23] which is based on a uniform strain. The calculated sets of elastic constants are given in Table 2 for both 'glitter' and 'neoglitter'.

All C_{ij} values are positive. Their combinations obeying the rules pertaining to the mechanical stability of the phase, and the equations providing bulk B_V and shear G_V moduli are as follows for the tetragonal system:

C_{ij} (i =1, 3, 4, 6) > 0; $C_{11} > C_{12}$, $C_{11} + C_{33} - 2C_{13} > 0$; and $2C_{11} + C_{33} + 2C_{12} + 4C_{13} > 0$.

$$B_{Voigt}^{tetr.} = 1/9\ (2C_{11} + C_{33} + 2C_{12} + 4C_{13});$$

$$G_{Voigt}^{tetr.} = 1/15\ (2C_{11} + C_{12} + 2\ C_{33} - 2C_{13} + 6C_{44} + 3C_{66}).$$

Both tetragonal C_6 phases have close C_{ij} values (see Table 2), however, for 'neoglitter' calculated B_V and G_V moduli are somewhat larger than those of 'glitter', but still smaller than moduli accepted for diamond i.e., B_V =445 GPa and G_V = 530 GPa (cf. [1] and references therein). Note that the statement that the systems under consideration are elastically stable implies that scaling the cell in any direction, without changing of the atoms coordinates, leads to an energy increase.

(ii) *Hardness*

Vickers hardness (H_V) was predicted using three modern theoretical models: (i) thermodynamic model based on crystal structure and thermodynamic properties [24], (ii) Lyakhov-Oganov model which considers the strength of covalent bonding, degree of ionicity and topology of the crystal structure [25] and empirical Chen-Niu model that uses the elastic properties [26]. The fracture toughness (K_{Ic}) was evaluated within Mazhnik-Oganov model [27].

Table 3 presents Vickers hardness and bulk moduli (B_0) calculated in the framework of thermodynamic model of hardness; other mechanical properties such as shear modulus (G), Young's modulus (E), the Poisson's ratio (ν) and fracture toughness (K_{Ic}) are given in Table 4. The density (ρ) is highest for diamond, followed by 'neoglitter' and then 'glitter', which is the least dense allotrope due to its more open structure. Bulk modulus values follow density, i.e., the higher the density, the lower the compressibility, and Young's moduli increase proportionally with shear moduli. With regard to hardness, as has been shown earlier, in the case of ultrahard compounds of light elements, the thermodynamic model shows surprising agreement with the available experimental data [29]. Moreover, its use is preferable in the case of hybrid dense carbon allotropes, for which Lyakhov-Oganov model gives underestimated hardness values whereas the empirical Chen-Niu model does not work at all. Since Vickers hardness of both 'glitter' and 'neoglitter' exceeds 80 GPa, they should be attributed to the family of ultrahard phases [30]. The higher hardness of 'neoglitter' is apparently due to the higher density.

Dynamic stability from the phonons.

Besides the structural stability criteria observed for 'neoglitter' from the positive magnitudes of the elastic constants and their combinations, another stability criterion is obtained from the phonons.

Fig. 4 shows the phonon bands of template C_4 (Fig. 4a) and neoglitter (Fig. 4b). Along the horizontal direction, the bands run along the main lines of the tetragonal Brillouin zone (reciprocal k-space). The vertical direction shows the frequencies given in units of terahertz (THz). Since no negative frequency magnitudes are observed, tet-C_6 is considered as dynamically stable. This is usually referred to as 'kinetically' stable, implying that all the atoms in the structure are trapped within local energy minima, meaning that they will remain in their respective positions at sufficiently low temperatures. Oppositely, a dynamically kinetically unstable structure, with

negative low energy acoustic frequencies, would be unstable and likely to undergo phase transition (or possibly melting) within a very short timescale ~10^{-9}s.

There are 3N-3 optical modes at higher energy than three acoustic modes that can be counted between Γ and R. They start from zero energy (ω = 0) at the Γ point, center of the Brillouin zone, up to a few terahertz. Acoustic modes describe the lattice rigid translation modes with two transverse modes and one longitudinal mode. For both C_4 and C_6 the remaining bands correspond to the optic modes culminating at ω = 40 THz, a magnitude close to the observed for diamond by Raman spectroscopy: ω ~ 40 THz [31]. However, for C_6 the high frequency arises probably due to rigid vibrations of trigonal C-C pairs.

Electronic band structures.

Fig. 5 shows the electronic band structure and the site projected density of states (DOS) of tet-C_6 obtained using the all-electrons DFT-based augmented spherical method (ASW) [32] using GGA exchange correlation functional [15]. In Fig. 5a the energy level along the vertical line is with respect to the Fermi level (E_F) crossed by bands with subsequent metallic behavior. The DOS shown beside the band structure (Fig. 5b) provide further interpretation for the electronic structure with the zero energy along the x-axis at E_F. The projected DOS along C1 (tetrahedral) and C2 (trigonal) sites show large similarities in the energy range {-20; -5 eV} ensuring for the chemical bonding between the two sites, but large differences appear above -5 eV and above E_F within the (empty) conduction band. The prevailing C2-DOS at E_F and the vanishingly small C1 magnitude of C1 DOS clearly show that the conductivity is selectively caused by trigonal carbon as discussed in the charge density subsection. Further support is also found from the weighted bands in Fig. 5c where the bold bands relative to C1 are found deeper in energy whereas C2 bands are found responsible of the states crossing E_F, thus responsible of the metallic character and resulting from the π-electrons having more itinerant behavior than the less extended σ electrons.

4. Conclusions

In the present work a novel ultrahard carbon allotrope, body-centered tetragonal C_6, was proposed with the particularity of presenting mixed sp^2-sp^3 carbon hybridizations featuring tetrahedral carbon in *C4* tetrahedra and the stacking of in-plane corner-sharing *C4* being connected by trigonal carbon. Mixed sp^2-sp^3 carbon systems are relevant as models upon considering modern investigations of nanodiamonds for electronic applications [33,34]. Further investigations of relevant model carbons with less sp^2 content are underway. The results of the investigation of relevant model carbons with a lower sp^2 content have recently been published [35].

REFERENCES

[1] V.V. Brazhkin, V.L. Solozhenko, Myths about new ultrahard phases: Why materials that are significantly superior to diamond in elastic moduli and hardness are impossible. *J. Appl. Phys.* **125** (2019) 130901.

[2] S. Zhang, J. He, Z. Zhao, D. Yu, Y. Tian, Discovery of superhard materials via CALYPSO methodology. *Chinese Phys. B* **28** (2019) 106104.

[3] A.R. Oganov, Crystal structure prediction: reflections on present status and challenges. *Faraday Discuss*. **211** (2018) 643.

[4] P. Hohenberg, W. Kohn, Inhomogeneous electron gas. *Phys. Rev. B* **136** (1964) 864-871.

[5] W. Kohn, L.J. Sham, Self-consistent equations including exchange and correlation effects. *Phys. Rev. A* **140** (1965) 1133-1138.

[6] SACADA **(**Samara Carbon Allotrope Database). www.sacada.info

[7] S.F. Matar, V.L. Solozhenko, The simplest dense carbon allotrope: Ultra-hard body centered tetragonal C_4. *J. Solid State Chem.* **314** (2022) 123424; S.F. Matar, V.L. Solozhenko, Corrigendum to "The simplest dense carbon allotrope: Ultra-hard body-centered tetragonal C_4" [J. Solid State Chem. 314 (2022) 123424]. *J. Solid State Chem.* **317** (2023) 123587.

[8] A.P. Shevchenko, A.A. Shabalin, I.Yu. Karpukhin, V.A. Blatov, Topological representations of crystal structures: generation, analysis and implementation in the TopCryst system. *STAM: Methods* **2** (2022) 250-265. https://topcryst.com

[9] M.J. Bucknum, R. Hoffmann, A hypothetical dense 3,4-connected carbon net and related B_2C and CN_2 nets built from 1,4-cyclohexadienoid units. *J. Am. Chem. Soc.* **116** (1994) 11456-11464.

[10] S.F. Matar, J. Etourneau, V.L. Solozhenko, Novel (super)hard SiCN from crystal chemistry and first principles. *Silicon* (2022), https://doi.org/10.1007/s12633-022-02033-7

[11] S.F. Matar, V.L. Solozhenko, New superhard tetragonal BCN from crystal chemistry and first principles. *Materialia* **26** (2022) 101581.

[12] G. Kresse, J. Furthmüller, Efficient iterative schemes for ab initio total-energy calculations using a plane-wave basis set. *Phys. Rev. B* **54** (1996) 11169.

[13] G. Kresse, J. Joubert, From ultrasoft pseudopotentials to the projector augmented wave. *Phys. Rev. B* **59** (1999) 1758-1775.

[14] P.E. Blöchl, Projector augmented wave method. *Phys. Rev. B* **50** (1994) 17953-17979.

[15] J. Perdew, K. Burke, M. Ernzerhof, The Generalized Gradient Approximation made simple. *Phys. Rev. Lett*. **77** (1996) 3865-3868.

[16] J. Heyd, G.E. Scuseria, M. Ernzerhof, Hybrid functionals based on a screened Coulomb potential. *J. Chem. Phys.* **124 (**2006) 219906.

[17] W.H. Press, B.P. Flannery, S.A. Teukolsky, W.T. Vetterling, *Numerical Recipes*, 2nd ed. Cambridge University Press: New York, USA, 1986.

[18] P.E. Blöchl, O. Jepsen, O.K. Anderson, Improved tetrahedron method for Brillouin-zone integrations. *Phys. Rev. B* **49** (1994) 16223-16233.

[19] M. Methfessel, A.T. Paxton, High-precision sampling for Brillouin-zone integration in metals. *Phys. Rev. B,* **40** (1989) 3616-3621.

[20] H.J. Monkhorst, J.D. Pack, Special k-points for Brillouin Zone integration. *Phys. Rev. B* **13** (1976) 5188-5192.

[21] A. Togo, I. Tanaka, First principles phonon calculations in materials science, *Scr. Mater.* **108** (2015) 1-5.

[22] V. Eyert, The Augmented Spherical Wave Method, Lect. Notes Phys. 849 (Springer, Berlin Heidelberg 2013).

[23] W. Voigt, Über die Beziehung zwischen den beiden Elasticitätsconstanten isotroper Körper. *Annal. Phys.* **274** (1889) 573-587.

[24] V.A. Mukhanov, O.O. Kurakevych, V.L. Solozhenko, The interrelation between hardness and compressibility of substances and their structure and thermodynamic properties. *J. Superhard Mater.* **30** (2008) 368-378.

[25] A.O. Lyakhov, A.R. Oganov, Evolutionary search for superhard materials: Methodology and applications to forms of carbon and TiO_2. *Phys. Rev.* B **84** (2011) 092103.

[26] X.Q. Chen, H. Niu, D. Li, Y. Li, Modeling hardness of polycrystalline materials and bulk metallic glasses. *Intermetallics* **19** (2011) 1275-1281.

[27] E. Mazhnik, A.R. Oganov, A model of hardness and fracture toughness of solids. *J. Appl. Phys.* **126** (2019) 125109.

[28] N. Bindzus, T. Straasø, N. Wahlberg, J. Becker, L. Bjerg, N. Lock, A.-C. Dippel, B.B. Iversen, Experimental determination of core electron deformation in diamond. *Acta Cryst. A* **70** (2014) 39-48.

[29] S.F. Matar, V.L. Solozhenko, Crystal chemistry and ab initio prediction of ultrahard rhombohedral B_2N_2 and BC_2N. *Solid State Sci.* **118** (2021) 106667.

[30] V.L. Solozhenko, Y. Le Godec, A hunt for ultrahard materials. *J. Appl. Phys.* **126** (2019) 230401.

[31] R.S. Krishnan, Raman spectrum of diamond. *Nature* **155** (1945) 171.

[32] V. Eyert, Basic notions and applications of the augmented spherical wave method. *Int. J. Quantum Chem.* **77** (2000) 1007-1031.

[33] Y. Lin, X. Sun, D.S. Su, G. Centi, S. Perathoner, Catalysis by hybrid sp^2/sp^3 nanodiamonds and their role in the design of advanced nanocarbon materials. *Chem. Soc. Rev.* **47** (2018) 8438-8473.

[34] Z. Zhai, N. Huang, X. Jiang, Progress in electrochemistry of hybrid diamond/sp^2-C nanostructures. *Curr. Opin. Electrochem.* **32** (2022) 100884.

[35] S.F. Matar, V. Eyert, V.L. Solozhenko, Novel ultrahard extended hexagonal C_{10}, C_{14} and C_{18} allotropes with mixed sp^2/sp^3 hybridizations: Crystal chemistry and ab initio investigations. *C — Journal of Carbon Research* **9** (2023) 11.

Table 1. Crystal structure parameters of two tetragonal carbon allotropes

Space group *I*-4*m*2 (N°119)		
	dia C_4 [7]	**tfa** C_6 'neoglitter'
a (Å)	2.53	2.47
c (Å)	3.57	6.43
C1	(2*a*) 0, 0, 0	(2*a*) 0, 0, 0
C2	(2*d*) ½, 0, ¼	(4*f*) 0, ½, 0.86
V (Å^3)	22.85	39.22
d_{C1-C2} (Å)	1.55	1.53
d_{C2-C2} (Å)	–	1.41

Table 2. Calculated elastic constants and bulk (B_V) and shear (G_V) moduli of two tetragonal C_6 allotropes

	C_{11}	C_{12}	C_{13}	C_{33}	C_{44}	C_{66}	B_V	G_V
'glitter'	715	45	95	1172	69	75	341	283
'neoglitter'	773	10	109	1296	132	298	366	375

Table 3 Vickers hardness (H_V) and bulk moduli (B_0) of carbon allotropes calculated in the framework of the thermodynamic model of hardness [24]

	Space group	$a = b$ (Å)	c (Å)	ρ (g/cm^3)	H_V (GPa)	B_0 (GPa)
'neoglitter' C_6	*I*-4*m*2	2.4666	6.4320	3.058	85	385
'glitter' C_6	$P4_2/mmc$	2.5899	5.9789	2.984	83	376
diamond	*Fd*-3*m*	3.5666 [28]	–	3.517	98	445 [1]

Table 4 Mechanical properties of carbon allotropes: Vickers hardness (H_V), bulk modulus (B), shear modulus (G), Young's modulus (E), Poisson's ratio (ν) and fracture toughness (K_{Ic})

	H_V			B		G_V	E [d]	ν [d]	K_{Ic} [e]
	T [a]	LO [b]	CN [c]	B_0 [a]	B_V				
	GPa								MPa·m^{½}
'neoglitter' C_6	85	78	63	385	366	375	839	0.118	4.7
'glitter' C_6	83	75	44	376	340	296	688	0.163	5.7
diamond	98	90	93	445 [f]		530 [f]	1138	0.074	6.4

[a] Thermodynamic model [24]

[b] Lyakhov-Oganov model [25]

[c] Chen-Niu model [26]

[d] E and ν values calculated using isotropic approximation

[e] Mazhnik-Oganov model [27]

[f] Ref. 1

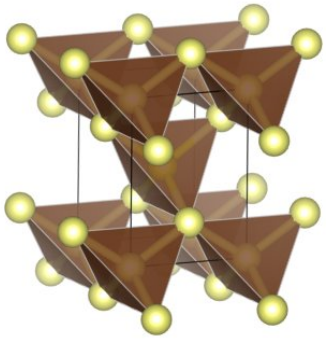

(*a*)

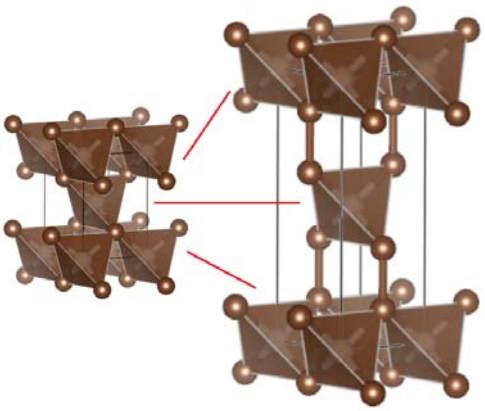

(*b*)

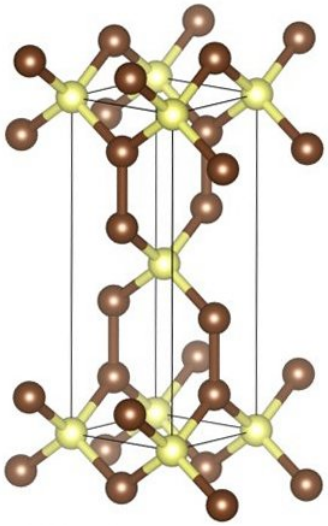

(*c*)

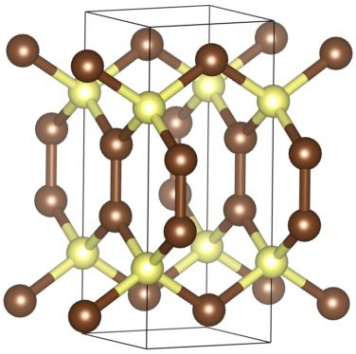

(*d*)

Figure 1. Template C_4 [7] (*a*) and C_4 → tet-C_6 transformation scheme (*b*) (tetrahedra highlighted); tet-C_6 'neoglitter' (*c*) and C_6 'glitter' [8] (*d*) (tetrahedral (sp^3) and trigonal (sp^2) carbons are shown by yellow and brown spheres, respectively).

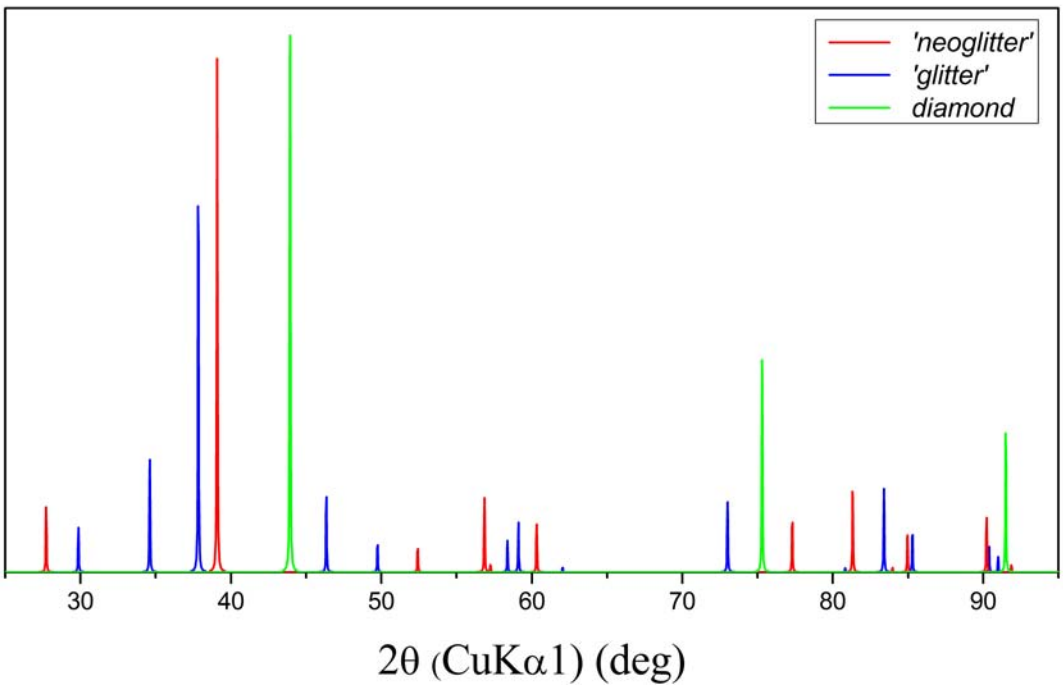

Figure 2 Simulated X-ray diffraction patterns of three dense carbon allotropes.

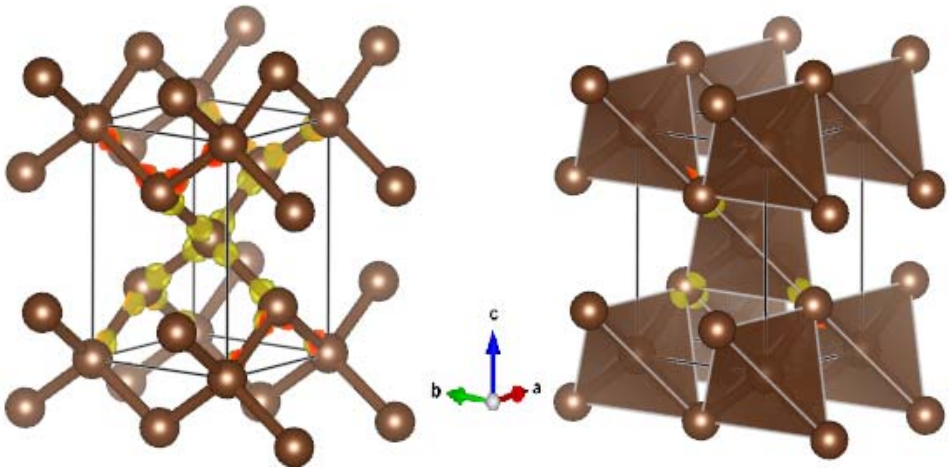

(*a*)

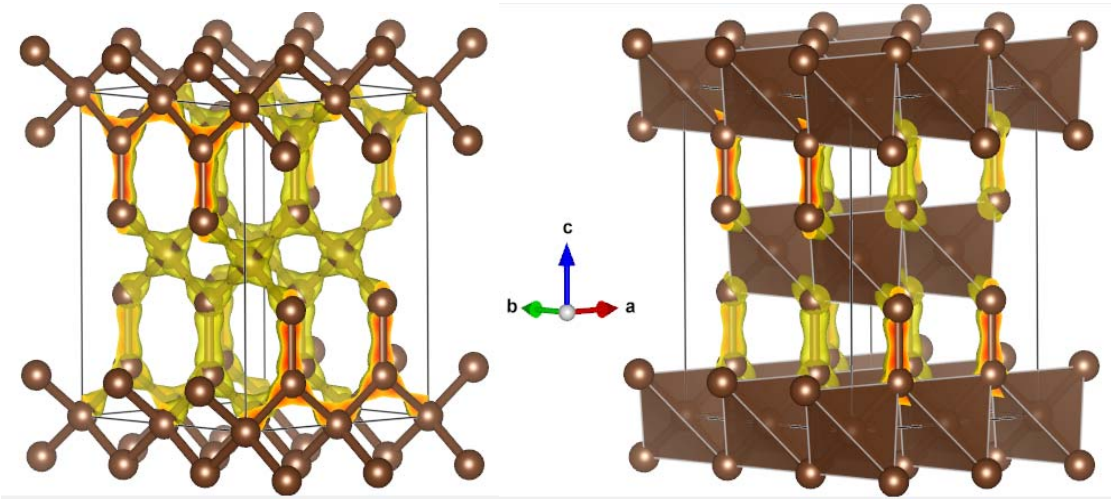

(*b*)

Figure 3. Sketches of the structures in extended cell presentation highlighting the charge density yellow volumes: template C_4 [7] (*a*) and body-centered tetragonal C_6 ('neoglitter') (*b*).

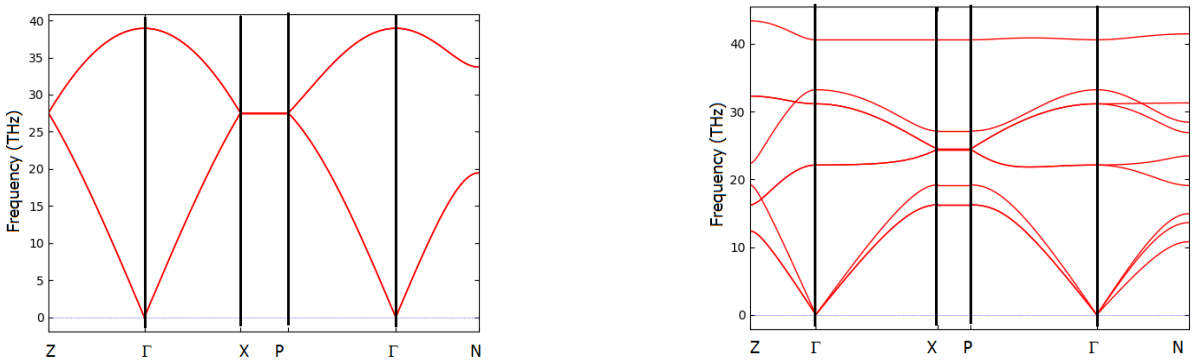

Figure 4. Phonon band structures of template body-centered tetragonal C_4 (*a*) and novel body-centered tetragonal C_6 ('neoglitter') (*b*)

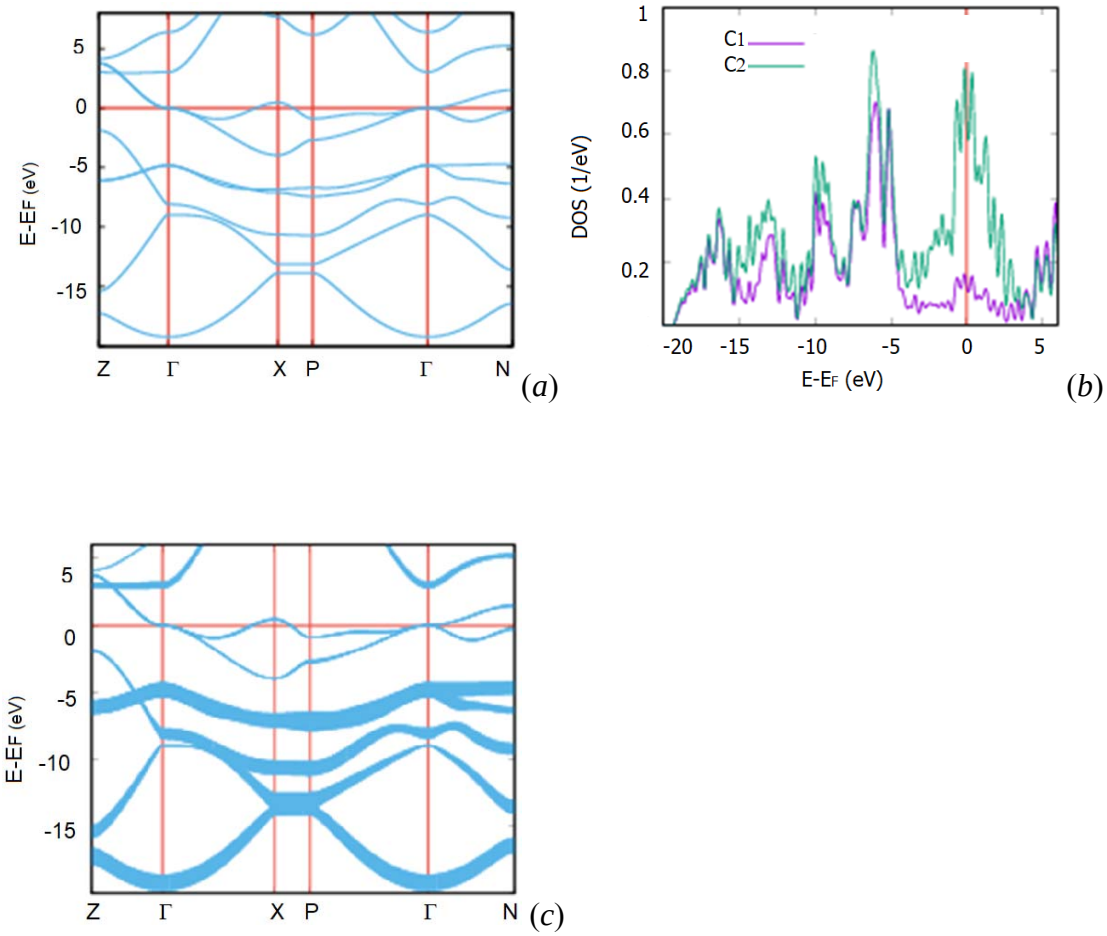

Figure 5. Body-centered tetragonal C_6 ('neoglitter'): electronic band structure (*a*) and site projected density of states (*b*). C1-weighted bands (bold stripes) show the prevalence of C1 diamond-like bands at lower energies; C2 bands cross E_F (*c*).